large influence of pH on the transient behavior, illustrated in Fig. 3.

Conclusions

Ferric oxide shows a rather complex photoelectrochemical behavior which is displayed by different types of transient behavior. This factor complicates its use as an electrode for semiconductor-liquid junction solar cells. However evidently the transient behavior is modified by sample preparation, and this provides an opportunity to suppress the back-reaction of the intermediate which is partly responsible for the low measured quantum yields.

Electrodes prepared by sintering very pure ferric oxide show the best results in this respect. The use of ferric oxide in solar cells is made particularly attractive by the fact that it can display exceptionally low flatband potentials.

Acknowledgments

We would like to acknowledge the assistance of Dr. R. Palinski who provided the sintered ferric oxide samples, and the technical assistance of Mr. A. Hoffmann and Mr. R. Schubert. We would also like to thank Dr. R. Memming for his extremely helpful comments during the course of this work.

Manuscript submitted July 6, 1978; revised manuscript received Aug. 8, 1978.

Any discussion of this paper will appear in a Discussion Section to be published in the December 1979 JOURNAL. All discussions for the December 1979 Discussion Section should be submitted by Aug. 1, 1979.

Publication costs of this article were assisted by Euratom.

REFERENCES

1. H. Gerischer, in "Special Topics in Electrochemistry," Elsevier Scientific Publishing Co., Amsterdam, The Netherlands (1977).
2. "Semiconductor Liquid-Junction Solar Cells," Proceedings of a Conference on the Electrochemistry and Physics of Semiconductor Liquid Interfaces under Illumination, held at Airlie, Virginia, May 3-5, 1977, A. Heller, Editor, The Electrochemical Society Softbound Symposium Series, PV 77-3, Princeton, N.J. (1977).
3. K. L. Hardee and A. F. Bard, *This Journal*, **123**, 1025 (1977).
4. R. K. Quinn, R. D. Nasby, and R. J. Baughman, *Mater. Res. Bull.*, **11**, 1011 (1976).
5. Lun-shu Ray Jeh and N. Hackerman, *This Journal*, **124**, 833 (1977).
6. J. H. Kennedy and K. W. Frese, Paper 328 presented at The Electrochemical Society Meeting, Philadelphia, Pa., May 8-13, 1977.
7. M. A. Butler, *J. Appl. Phys.*, **48**, 1914 (1977).
8. J. G. Mavroides, in "Semiconductor Liquid-Junction Solar Cells," Proceedings of a Conference of the Electrochemistry and Physics of Semiconductor Liquid Interfaces under Illumination, held at Airlie, Virginia, May 3-5, 1977, A. Heller, Editor, The Electrochemical Society Softbound Symposium Series, PV 77-3, p. 84, Princeton, N.J. (1977).
9. D. Pavlov, S. Zanova, and G. Papazov, *This Journal*, **124**, 1523 (1977).
10. D. M. Smyth and G. A. Shirn, *ibid.*, **115**, 187 (1968).
11. L. Peter, Private communication.
12. R. Memming, Private communication.
13. H. Gerischer, *This Journal*, **113**, 1174 (1966).
14. W. Gissler and R. Memming, *ibid.*, **124**, 1711 (1977).
15. D. M. Tench and G. Gerischer, *ibid.*, **124**, 1612 (1977).
16. F. Möllers, H. J. Tolle, and R. Memming, *ibid.*, **121**, 1160 (1974).

Semiconductor Electrodes

XVI. The Characterization and Photoelectrochemical Behavior of n- and p-GaAs Electrodes in Acetonitrile Solutions

P. A. Kohl* and A. J. Bard**

Department of Chemistry, University of Texas at Austin, Austin, Texas 78712

ABSTRACT

The photoelectrochemical behavior of n-type and p-type GaAs is investigated in acetonitrile solutions containing various redox couples. The cyclic voltammograms of the semiconductor electrodes in the dark and illuminated with red light are compared to the Nernstian behavior at a Pt disk electrode. The photodissolution of the semiconductors was surpressed and did not occur until potentials well positive of the flatband potential. An underpotential (negative overpotential) was developed on the photoassisted oxidation (n-type semiconductor) and reduction (p-type material) of solution species. Intermediate levels or surface states are shown to be capable of mediating electron transfer and limiting the magnitude of the underpotential produced. It is also shown that the production of surface films at potentials negative of the conduction bandedge can produce a photovoltaic effect with the GaAs assisting in electron transfer. Thus, photoassisted electron transfer with electroactive solution species is observed spanning a potential range greater than 2.5V utilizing a 1.35 eV photon.

Although the nature of charge transfer reactions at the semiconductor liquid interface can be broadly described by the Gerischer band theory (1), studies on a number of semiconductor electrodes immersed in both aqueous and nonaqueous solutions have shown that account must also be taken of surface states and intermediate levels, as well as changes in the nature of the surface during electrochemical studies that are specific to the semiconductor material and solvent. The latter effects are particularly important with small bandgap semiconductors which tend to be rather easily reduced or oxidized. Such surface effects are also of importance in photoelectrochemical cells (PEC) for the conversion of light energy to chemical and/or electrical energy and result in quantum efficiencies which vary with time, photocorrosion, passivation of

* Electrochemical Society Student Member.
** Electrochemical Society Active Member.

Downloaded 16 Feb 2009 to 146.6.143.190. Redistribution subject to ECS license or copyright; see http://www.ecsdl.org/terms_use.jsp

the electrode surface, and development of surface layers which can affect the observed photopotential. Surface pretreatments (*e.g.*, polishing, chemical etching) have been shown to affect the photoelectrochemical behavior of semiconductor electrodes, *e.g.*, GaAs (2, 3) and CdS (4), and hence can change the quantum and power efficiencies for the conversion of light in PEC's.

In this work the photoelectrochemical behavior of n- and p-GaAs in acetonitrile (ACN) solutions containing various one-electron reversible redox couples is described. An aprotic solvent is particularly useful, as discussed in previous papers (5, 8), because it has a large working potential range (or effective solvent bandgap) compared to water and can be employed to investigate potential regions which cannot be probed in aqueous solutions. Moreover, many stable redox couples exist in ACN, which show reversible electrochemical behavior over a wide range of redox potentials ($E°$). The rate of photodecomposition of semiconductors in ACN is often smaller because of the decrease in solvation of the products of photodissolution. Thus, n-CdS, n-GaP, and n-ZnO have been shown to be stable photoanodes in ACN and the results in ACN have also produced possible mechanistic information on factors affecting the stability of these materials when used as photoanodes in aqueous solutions (5). A previous paper from this laboratory (7) showed that the extent of passivation of n- and p-Si caused by film formation in aqueous solutions can be decreased in ACN. However, only small and transient underpotentials (negative overpotentials) were developed under irradiation for electron transfer with solution species (7).

Previous studies of GaAs (9-12), whose small bandgap (E_g), 1.35 eV, allows absorption of an appreciable portion of the solar spectrum, have shown that photoassisted electron transfer reactions can occur in aqueous solutions. We describe here the electrochemical behavior of both n- and p-type GaAs in ACN solutions in the dark and under irradiation. The location of the conduction band (CB) and valence band (VB) edge energies by determination of the flatband potential (V_{fb}) and the mapping of the bandgap region are described. We show that the behavior can be discussed in terms of the previously proposed model but that specific surface effects also play a major role.

Experimental

The high conductivity single crystal semiconductors used were provided with ohmic contacts (13) and mounted in glass tubes with the back and sides of the crystals insulated from solution as described previously (14). The n-GaAs obtained from Monsanto Corporation (St. Louis, Missouri), and p-GaAs, purchased from Atomergic Chemicals (Long Island, New York), were oriented with the (111) face exposed to solution. High purity polycrystalline GaAs slices (ROC/RIC, Sun Valley, California) were heated in a nitrogen atmosphere at 450°C for 4 hr with In and Ga vapor passed over the crystal. Electrodes of the resulting p-type conductivity material ($1 \times 2 \times 0.1$ cm) were prepared by the procedure used for the single crystals. The semiconductors were first mechanically polished with 0.5 μm alumina and then etched by one of the following procedures (the effect of the different pretreatments is discussed in the next section): (A) No chemical etchant; (B) 6*M* HCl for 30 sec; (C) H_2SO_4: H_2O_2:H_2O (3:1:1 by volume) for 10 sec; (D) the etchant in (C) for 5 sec followed by 6*M* HCl for 25 sec; (E) 5% Br_2 in methanol for 30 sec.

The ACN and compounds used were purified, dried, and characterized as described previously (5, 6). Polarographic grade *tetra-n*-butylammonium perchlorate (TBAP), which was dried for three days under vacuum, was used as the supporting electrolyte. A cyclic voltammogram at a Pt disk electrode was obtained at the beginning and end of each experiment to insure the purity of all chemicals used and calibrate the reference electrode potential.

A three-compartment electrochemical cell of previous design (6) was used. The counterelectrode was a coiled Pt wire separated by a medium porosity glass frit. The quasireference electrode was a silver wire immersed in the solution and separated from it by a medium porosity glass frit. All values are reported *vs.* the aqueous saturated calomel electrode (SCE). The half-wave potential of the TMPD/TMPD$^{+\cdot}$ redox couple was found in this study to be slightly negative of that reported previously (5, 6) when compared to the positions of the other redox couples. A large area (14 cm^2) Pt foil counterelectrode was used without a glass frit for capacitance measurements.

A PAR 173 potentiostat and PAR 175 Universal programmer (Princeton Applied Research Corporation, Princeton, N. J.) were used to obtain the cyclic voltammograms. Positive feedback was used to compensate for solution resistance and the internal resistance of the semiconductors. The i-V curves were recorded on a Houston Model 2000 X-Y recorder (Houston Instruments, Austin, Texas) for sweep rates less than or equal to 1 V/sec. For sweep rates greater than 1 V/sec a Model 1090A digital oscilloscope (Nicolet, Madison, Wisconsin) was used. The light source was a 450W xenon lamp (Oriel Corporation, Stamford, Connecticut) equipped with a red filter. The solutions were prepared and sealed in a helium-filled Vacuum Atmosphere Corporation (Hawthorne, California) glove box.

Results

Capacitance measurements.—The production of a depletion layer within the semiconductor leads to a change in the space charge capacitance as given by the Schottky-Mott (S-M) equation (Eq. [1])

$$1/C_{sc}^2 = 2(\Delta\phi_s - kT/e)/(\epsilon\epsilon_0 e n_o) \quad [1]$$

where C_{sc} is the space charge capacitance of the semiconductor, ϵ is the dielectric constant of the semiconductor, ϵ_0 is the permittivity of free space, n_o is the dopant concentration, and $\Delta\phi_s$ is the amount of band bending within the semiconductor. A plot of $1/C_{sc}^2$ *vs.* V should have a slope related to the donor (n-type) or acceptor (p-type) density and an x-intercept corresponding to V_{fb}. However, numerous studies of the variation of C_{sc} with V at different frequencies, such as those by Gomes *et al.* (15-17), have shown that nonlinearities and variations in the x-intercept of the S-M plots occur as a function of frequency. These frequency-dependent deviations introduce uncertainties in the extrapolated V_{fb} values and the slope-derived dopant densities. However, GaAs appeared to be particularly well-behaved in S-M plots at different frequencies in aqueous solutions and reasonable values of V_{fb} have been obtained with both the p- and n-type dopants (16-18). Similar consistent and well-behaved $1/C_{sc}^2$ *vs.* V plots were found in ACN with 0.5M TBAP as the supporting electrolyte. The total cell capacitance was measured from the charging current in the cyclic voltammograms at scan rates from 0.2 to 1000 V/sec as in Eq. [2] (14)

$$C_{sc} \approx C_{TOTAL} = i/vA \quad [2]$$

where C_{TOTAL} is the total capacitance measured, i is the nonfaradaic charging current, v is the scan rate, and A is the electrode area. The faradaic current was less than 1 $\mu A/cm^2$ and V_{fb} was found to be -1.0 and $+0.1V$ ($\pm 0.2V$) for n- and p-GaAs, respectively, etched by procedure (D) as shown in Fig. 1(a and b). The donor concentration (n_o) for n-GaAs and acceptor concentration (p_o) for p-GaAs were found to be $2 \times 10^{18}/cm^3$ (compared to manufactured specifications of $1.34 \times 10^{18}/cm^3$) and $3 \times 10^{18}/cm^3$, respectively. However, it was found that after repeated etchings by procedure (C) the V_{fb} shifted in a negative direction as shown in Fig. 1(c and d). Prolonged treatment in

Downloaded 16 Feb 2009 to 146.6.143.190. Redistribution subject to ECS license or copyright; see http://www.ecsdl.org/terms_use.jsp

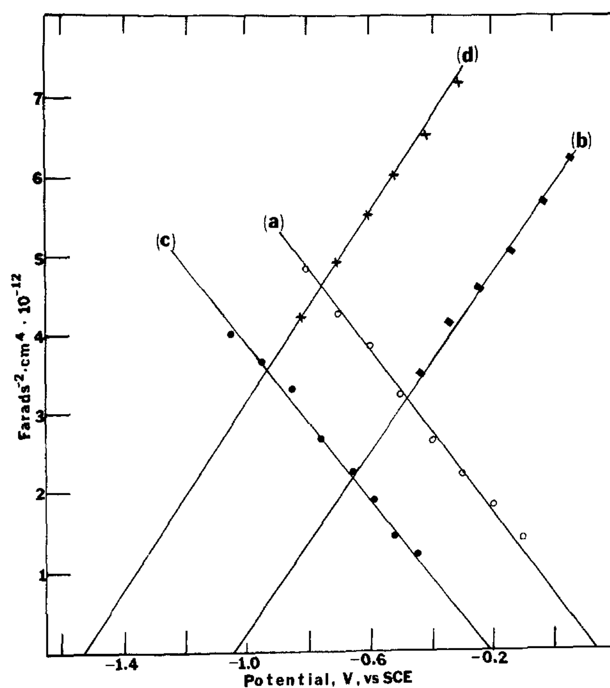

Fig. 1. Schottky-Mott plot in acetonitrile solution of 0.5M TBAP supporting electrolyte from cyclic voltammogram at 100 V/sec. (a) p-GaAs etched by procedure D, (b) n-GaAs etched by procedure D, (c) p-GaAs etched by method C, and (d) n-GaAs etched by procedure C.

the $H_2SO_4/H_2O_2/H_2O$ etchant produced a multicolored streaky looking surface which gave rise to nonlinear $1/C_{sc}^2$ *vs.* V plots.

Frequency dependence, or in this case scan rate dependence, was observed in the $1/C_{sc}^2$ *vs.* V plots with higher sweep rates producing steeper slopes and in most cases different x-intercepts. The frequency-dependent deviations were quite reproducible for a given etchant procedure and relatively small compared to the deviations observed with surface pretreatment. The etchant-related deviations in the Schottky-Mott plots correlated closely with the redox behavior of the crystals as will be discussed.

The V_{fb} was also estimated from the open-circuit photovoltage (19). If the potential of an n-type semiconductor electrode is adjusted positive of V_{fb} producing positive band bending, and then illuminated with light of energy greater than the bandgap, the photogenerated holes and electrons are separated in such a way as to decrease the electric field in the space charge layer. The net effect is that the open-circuit potential pulses in a negative direction toward V_{fb} under pulsed illumination. Experiments of this type with n-GaAs, using a battery to set the extent of band bending, produced negative potential pulse at all potentials from 0 to -2.6V. The p-type semiconductors should produce positive-going potential pulses when illuminated at potentials negative of V_{fb}. With p-GaAs positive pulses were seen from -2.6 to $+0.2$V.

Redox behavior.—The cyclic voltammetric (cv) behavior of the semiconductors was examined in the ACN solutions containing various redox couples. The dark peak currents, i_p, were directly proportional to $v^{1/2}$ in all cases for the scan rates (0.05-2 V/sec) and concentrations (0.2-5 mmole) employed. The current decay following the cv peaks showed approximately $t^{-1/2}$ decay. Thus the dark currents in these cv experiments was in all cases limited by the diffusion of the electroactive species in solution.

n-GaAs.—The electrochemical behavior of n-GaAs in ACN in the absence of added redox couples is shown in Fig. 2. The GaAs was etched by procedure (D) as described in the experimental section for all cv experiments unless noted otherwise. The initial scan from 0.0V to negative potentials shows a reduction peak at -1.5V which was not observed on a Pt disk electrode. The oxidation of the n-GaAs did not occur until the potential was positive of the valence bandedge both in the dark and when illuminated with red light even though the photodissolution of n-GaAs occurs positive of -0.7V in aqueous solutions. Small anodic current spikes (< 20 μA/cm^2), which decayed quickly with time, were observed when the electrode was illuminated with pulsed light at potentials positive of V_{fb} (-1V). The reduction of the solvent on n-GaAs electrode in the dark and when illuminated occurred at potentials more negative (-3.0V) than observed on a Pt disk electrode (-2.5V).

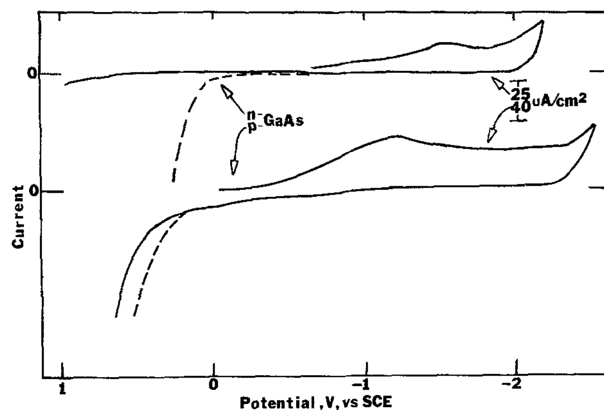

Fig. 2. The cyclic voltammogram in 0.1M TBAP solution at 0.2 V/sec in the dark (—) and illuminated (– – – –) of (a) n-GaAs and (b) p-GaAs.

Electron transfer between an n-type semiconductor and redox couples located at potentials negative of the CB edge should ideally resemble that at a metal, since the dark redox processes occur under accumulation layer conditions and no photoeffects (other than those attributable to heating and convection) are expected at these potentials. Such behavior has been observed previously with n-CdS, n-ZnO (5), and n-TiO_2 (6). However, deviations from this metal-like behavior were found for n-GaAs for all redox couples with standard potentials negative of V_{fb}. The dark reductions occurred at more negative potentials than at Pt and the anodic peak on reversal was located at more positive values with the difference in peak potentials, ΔE_p, being much larger than that expected for a reversible cv wave. For example, ΔE_p for the reduction of 9,10-diphenylanthracene (DPA) in the dark (Fig. 3) is much larger than on Pt. Under illumination the reduction and oxidation waves are both shifted to more negative potentials with a decrease in ΔE_p. The negative shift of the anodic wave under illumination results in the oxidation of the reduced forms occurring more easily (*i.e.*, at less positive potentials) at the illuminated n-GaAs than on Pt. The intensity-dependent reoxidation peak could be shifted to potentials even more negative than that of the reduction peak on n-GaAs, when the switching potential was sufficiently negative as shown. Etching procedure (B) produced a smaller photoeffect and yielded about the same peak potentials in the dark and under illumination. Peak potentials for various couples at Pt and GaAs are summarized in Table I.

The cv reduction of other couples with reductions occurring negative of V_{fb} showed similar behavior. Anthracene (A) reduction occurs in the dark with E_{pc} well negative of its value on Pt (Fig. 4). The oxidation of the radical anion in the dark on scan reversal occurs at much more positive potentials, *i.e.*, about -0.06 ($\pm$0.3)V. If the scan is again reversed following this anodic peak, the anodic current remains larger than that during the first reversal scan. This results in a crossing of the i-V curves (or hysteresis). Such be-

Downloaded 16 Feb 2009 to 146.6.143.190. Redistribution subject to ECS license or copyright; see http://www.ecsdl.org/terms_use.jsp

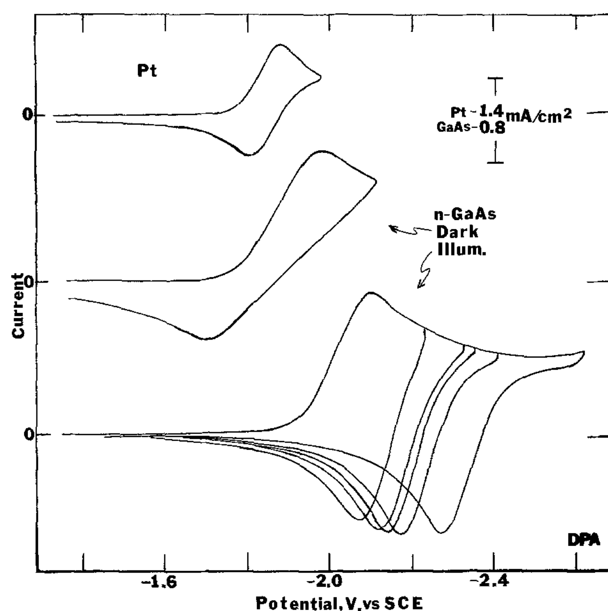

Fig. 3. Cyclic voltammogram of diphenylanthracene at a Pt disk electrode and single crystal n- and p-GaAs electrode in the dark and illuminated with red light. The DPA concentration was 2.3 mmoles and the scan rate was 0.2 V/sec.

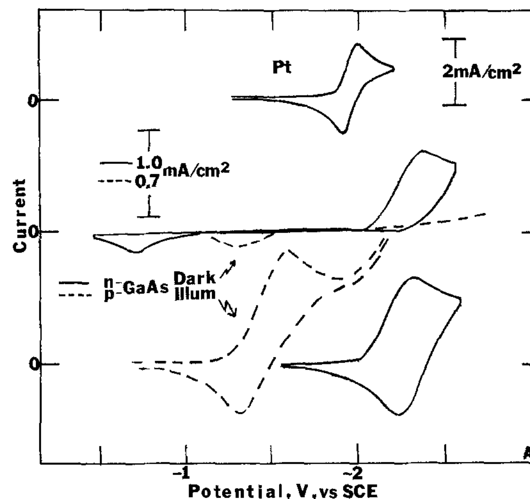

Fig. 4. Cyclic voltammogram of a 2.7 mmoles solution of anthracene at a Pt disk electrode and single crystal n-GaAs electrode in the dark and illuminated with red light. The scan rate was 0.2 V/sec.

havior in cv scans usually signals a change in the nature of the electrode surface. Irradiation of the n-GaAs with red light causes the reoxidation peak for $A^{\bar{\cdot}}$ to be shifted to potentials more negative than those observed on a Pt disk (Fig. 4). An open-circuit photopotential of 500 mV was measured between the illuminated n-GaAs and a Pt electrode in an equimolar $A/A^{\bar{\cdot}}$ solution. The anodic peak potential was dependent on the light intensity with the higher intensities shifting the peak to more negative potentials. Repetitive scans of the reduction and photooxidation peaks produced identical *i*-*V* curves for at least 100 scans. The reduction of the solvent was again shifted from its value on Pt to more negative potentials (*i.e.*, −3V). Such negative overpotentials under illumination have not been observed previously at an n-type semiconductor for couples negative of V_{fb}. They occur with a number of couples at n-GaAs, however, as shown by the data summarized in Fig. 5. The observed hysteresis and influence of etching procedure on the results strongly suggest that this effect is associated with changes in the GaAs surface in this potential region.

The three-step reversible reduction of $Ru(bipy)_3^{+2}$ to the anion provides further evidence of the changes in the n-GaAs surface. The reoxidation of $Ru(bipy)_3^{+}$ appears more reversible (*i.e.*, E_{pa} occurs at more negative potentials) when the potential scan is reversed directly after the first reduction peak and the scan is not extended to include the remaining two reduction waves. In this case E_{pa} for $Ru(bipy)_3^{+}$ occurs at −1.26V with a switching potential (E_λ) of −1.47V and not the −0.93V shown in Table I (obtained with E_λ = −2.2V). A similar effect is observed for the E_{pa} of $Ru(bipy)_3^{\circ}$, where E_{pa} is −1.44V, when E_λ = −1.62V. Each of the three intensity-dependent photooxidations were shifted to potentials negative of where they occur on a Pt disk electrode. Just as a more negative switching potential produced a more irreversible dark oxidation, it also produced a negative shift in the photooxidation peak potential. Each of the three photooxidation peaks for the oxidation of $Ru(bipy)_3^{-}$ to $Ru(bipy)_3^{2+}$ was shifted ~0.4 negative of their value on a Pt disk electrode. Thus, a similar underpotential was observed covering about a 1V range. The dark

Table I. Peak potentials for reductions and reoxidations of the compounds used in this study at the semiconductor electrodes in the dark and illuminated with red light. All potentials are vs. SCE and at a scan rate of 0.2 V/sec*

		n-GaAs				p-GaAs			
		Dark		Illuminated		Dark		Illuminated	
	E†	E_{pc}	E_{pa}	E_{pc}	E_{pa}	E_{pc}	E_{pa}	E_{pc}	E_{pa}
Bandgap		1.35eV				1.35eV			
V_{fb}		−1.0V (±0.2)				+0.1V (±0.2)			
A	−1.94	−2.45	−0.06	−2.32	−2.29	—	−1.3	−1.6	−1.42
DPA	−1.84	−1.97	−1.69	−2.09	−2.27	—	−1.6	−1.59	−1.58
$Ru(bipy)_3^{+2}$	−1.30	−1.38	−0.93	−1.44	−1.65	−2.12	−0.79	−0.72	−0.74
	−1.49	−1.55	−1.37	−1.62	−1.79	−2.27	—	−0.85	−0.89
	−1.73	−1.84	−1.79	−2.06	−2.08	—	—	−1.08	−1.04
$Ru(TPTZ)_2^{+3}$	−0.81	−0.88	—	−0.99	−1.23	−2.06	−0.62	−0.37	−0.52
	−0.97	−1.05	0.5	−1.17	−1.38	—	—	−0.53	−0.70
	−1.63	−1.73	−1.59	−1.88	−1.92	—	—	−1.07	−1.15
	−1.88	−2.0	−1.88	−2.18	−2.12	—	—	−1.27	−1.27
AQ	−0.94	−1.64	0.9	−1.54	−1.44	−2.4	−0.62	−0.65	−0.52
BQ	−0.52	−1.47	—	−1.45	−0.98	−2.4	−0.17	−0.68	−0.42
$Ox\text{-}1^{\dot{+}}$	−0.42	−0.75	—	−0.93	−0.98	−0.60	−0.35	−0.3	−0.25
		−1.66	—	−1.69	−1.74	−2.4	−1.05	−1.0	−0.95
$TMPD^{\dot{+}}$	0.1	−0.62	—	−0.61	−0.42	0.02	0.16	0.12	0.24
						0.61	0.70	0.63	0.78

* Abbreviations used in this table: A, anthracene; DPA, diphenylanthracene; bipy, bipyridine; TPTZ, 2,4,6-tripyridyl-s-triazene; AQ, anthraquinone; BQ, benzoquinone; Ox-1, oxazine-1; TMPD, N,N, N′, N′, tetramethyl-p-phenylenediamine.
† The reversible redox potential on a PT disk electrode.

Downloaded 16 Feb 2009 to 146.6.143.190. Redistribution subject to ECS license or copyright; see http://www.ecsdl.org/terms_use.jsp

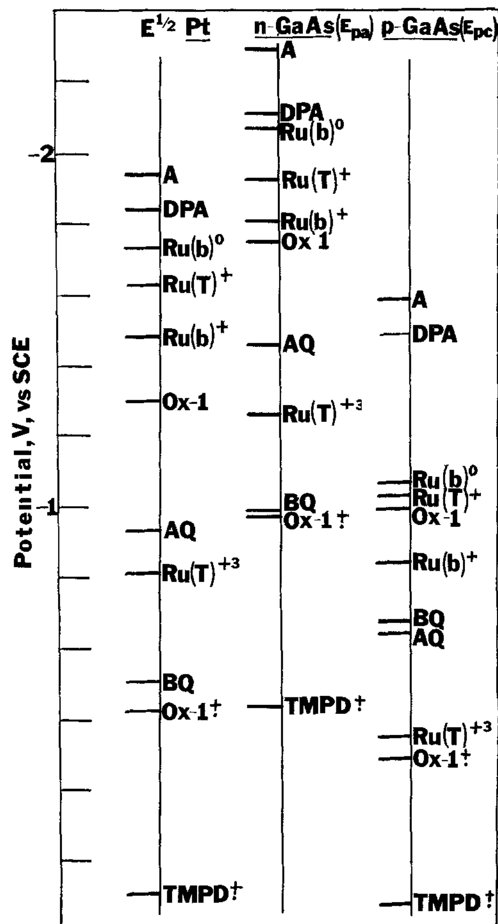

Fig. 5. The peak potentials of the photooxidations on n-GaAs and photoreductions on p-GaAs from Table I.

reduction peaks of $Ru(bipy)_3{}^{+2}$ were shifted to more negative potentials after pretreatment (C), however, no underpotential was observed for the photooxidation peaks. The photooxidation peaks after pretreatment (E) were not shifted to as negative potentials as with treatment (D).

Similar cv behavior in the dark and under illumination was observed with anthraquinone (AQ) and $Ru(TPTZ)_2{}^{3+}$, both of which are reduced at Pt at potentials near V_{fb} of n-GaAs. The cv dark reduction of AQ to the red radical anion occurred at potentials about 0.7V negative of the reduction at Pt (Fig. 6) and the i-V curves showed some hysteresis at scan rates greater than 0.5 V/sec (*i.e.*, the reduction current at the foot of the reduction peak was smaller than the reduction current at the same potential following scan reversal after the cathodic peak). On an initial scan, the photooxidation peak potential occurred at about −1.23V, when E_λ was more negative than −1.5V. However, if E_λ was extended to −2.8V, then the dark cathodic peak and photoanodic peaks were shifted to more negative potentials shown in Fig. 6. The nature of the i-V curves depended strongly on the electrode pretreatment. Procedure (B) produced more reversible peaks in the dark and a smaller underpotential. Etchant (C) caused the reduction to shift to more negative potentials (∼ −1.9V) and decreased the photooxidation current at potentials negative of −1V, while treatment (E) produced i-V curves similar to those found with (B), with E_{pc} and E_{pa} at −1.36 and −1.18V, respectively, under illumination.

The reversible four-step reduction of $Ru(TPTZ)_2{}^{+3}$ to the anion appeared more reversible on n-GaAs when the E_λ was set at more positive potentials, similar to the behavior found with $Ru(bipy)_3{}^{+2}$. Photooxidations of each oxidation state were observed with photoeffects observed over a potential range larger than E_g (Fig. 5).

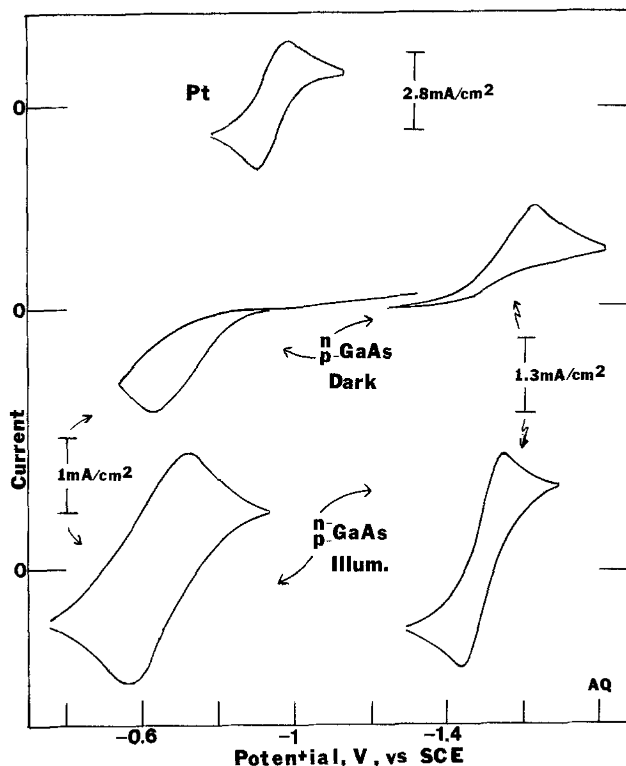

Fig. 6. Cyclic voltammogram of a 3 mmoles AQ, 3 mmoles AQ· solution at a Pt disk electrode and at a n- and p-GaAs single crystal electrode in the dark and illuminated with red light. The scan rate was 0.2 V/sec.

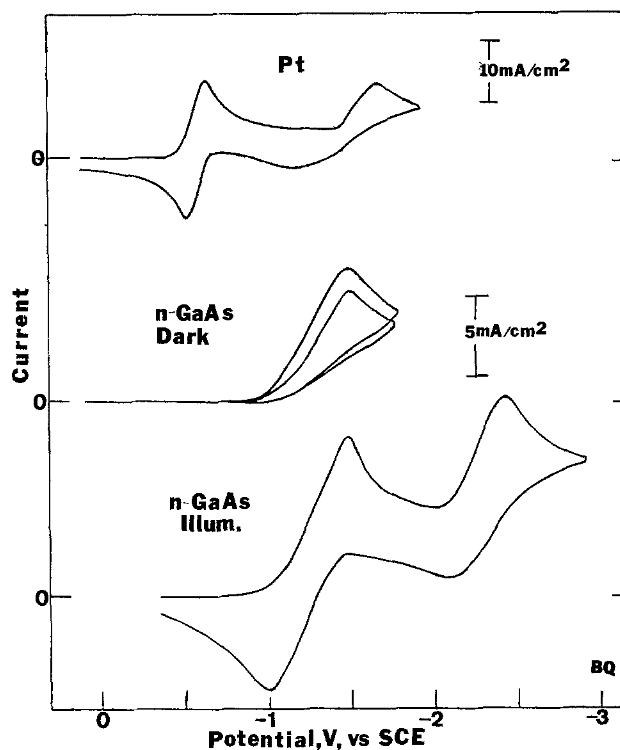

Fig. 7. Cyclic voltammogram of a 10 mmoles BQ, 10 mmoles BQ· solution at a Pt disk electrode and n-GaAs single crystal electrode in the dark and illuminated with red light. The scan rate was 0.2 V/sec.

Couples with potentials located within the bandgap showed cv behavior closer to that observed with other semiconductor electrodes, although the etching pretreatment still was of importance. The cv curves for the irreversible reduction of BQ to the radical anion on n-GaAs are shown in Fig. 7. The wave is shifted al-

Downloaded 16 Feb 2009 to 146.6.143.190. Redistribution subject to ECS license or copyright; see http://www.ecsdl.org/terms_use.jsp

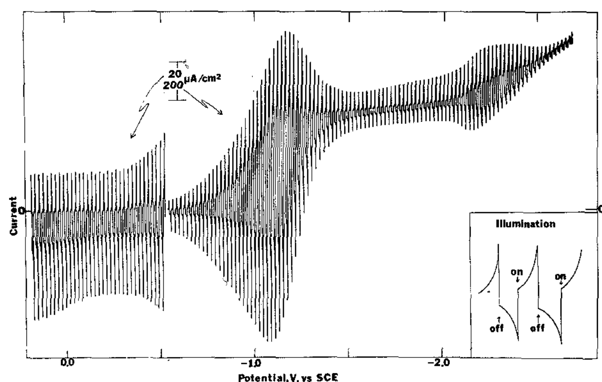

Fig. 8. Potential sweep of a 2.25 mmoles BQ solution at a single crystal n-GaAs electrode pulsed with red light as shown in inset. The sweep toward positive potentials at 10 mV/sec.

most 1V negative of its position at Pt and no oxidation wave on reversal is seen in the dark. Under illumination a photoanodic current following reversal at -0.98V was observed. The effect of periodic illumination during a linear scan toward positive potentials is shown in Fig. 8. Note that in this case, as opposed to similar experiments reported at other semiconductors (5), a photoeffect is observed at potentials well negative of V_{fb}. In the region of the BQ reduction wave the photocurrent decay is proportional to $t^{-1/2}$ and cathodic overshoots during the dark periods, representing reduction of BQ photogenerated during the light pulse, are observed. At potentials positive of -1.1V the height of these overshoots decreases because BQ reduction no longer occurs as readily and the oxidized form (BQ) builds up at the electrode surface. However small cathodic overshoots are still observed up to the foot of the BQ reduction wave. The magnitude of the cathodic overshoots decreased to the background levels observed without BQ present at potentials positive of -0.5V where reduction of BQ does not occur on Pt. The steady-state current observed under continuous irradiation at a given potential is a function of photon flux at the electrode surface, and the rate of back-reduction reaction which produces a specific concentration profile is discussed in the next section. Etchant (B) produced more reversible dark currents and treatment (C) produced more irreversible peak separations; smaller photoeffects were observed with both of these treatments. Etchant (E) produced results similar to (D) but the photoanodic peak potential was slightly more positive (-0.84V). The dark reduction of Ox-1$^{\dot{+}}$ ($E^\circ = -0.42$V) was also irreversible on n-GaAs positive of V_{fb}. The reduction and photooxidation peak potentials, given in Table I, depended on the electrode pretreatment procedure. TMPD$^{\dot{+}}$ was also irreversibly reduced on n-GaAs positive of V_{fb} as shown in Fig. 9. The photooxidation of TMPD to the blue radical cation also occurred with E_p well positive of V_{fb} and with an underpotential of $\sim$0.5V. When the flux of photogenerated holes exceeded the flux of TMPD to the electrode surface, a current peak was observed which shifted to more positive potentials on subsequent scans. However, when the flux of TMPD exceeded the flux of holes, a photoanodic current plateau at a given potential was observed which was stable for several hours of continuous current flow.

The reduction and reoxidation peak potentials of solution species whose E° lies within the bandgap thus show redox behavior similar to that previously observed in ACN where electron transfer via intermediate energy levels was proposed (5-7). A model neglecting states in the gap (1) predicts that the reduction current should be proportional to the concentration of electrons at the CB edge and density of states of oxidized species at that energy in solution. However, the potential-dependent reduction which occurred at the most positive potential was that of TMPD$^{\dot{+}}$ whose overlap with the CB energy levels is the smallest of those species lying below the CB edge. The reduction of TMPD$^{\dot{+}}$ occurred at potentials well positive of V_{fb} (-1V), probably via some intermediate level mechanism. Thus, the magnitude of the underpotential for the photooxidation of TMPD is limited by the rate of reduction (or back-reaction).

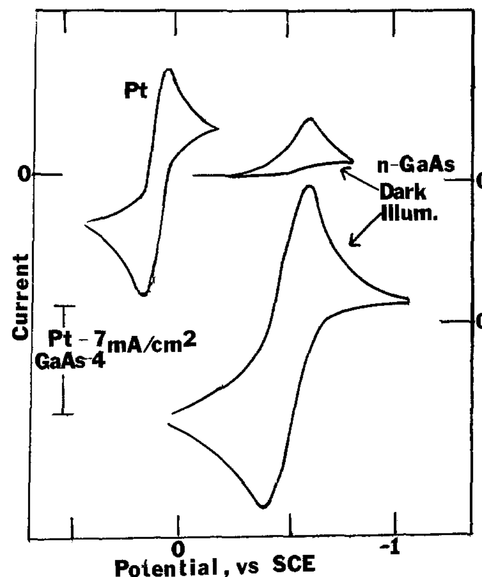

Fig. 9. Cyclic voltammogram of a 15 mmoles TMPD, 10 mmoles TMPD$^{\dot{+}}$ solution at a Pt disk electrode and n-GaAs single crystal electrode in the dark and illuminated with red light. The scan rate was 0.2 V/sec.

p-GaAs.—The cv curves of p-GaAs in an ACN solution containing only supporting electrolyte, shown in Fig. 2b, show currents attributable to dissolution of the electrode at potentials positive of 0V both in the dark and under illumination. A small dark cathodic peak was observed at -1V while the background photoreduction occurred at about -2V compared to -2.5V on a Pt disk electrode. For a p-type semiconductor, in the absence of surface states or intermediate levels, redox couples lying within the bandgap region should be oxidized in the dark at potentials more positive than V_{fb} (near the valence bandedge) while photoreductions should occur at potentials negative of V_{fb}. Those redox couples located above the CB edge (*i.e.*, at potentials more negative than about -1.0V), which have significant overlap of the reduced species with the CB energy levels, are not expected to undergo photoreduction at potentials more positive than at a Pt electrode, because (*i*) the potential or reducing power of the photogenerated electron in the CB is not great enough to fill a vacant energy level in such a solution species and (*ii*) the rate of oxidation (*i.e.* back-reaction) of the photogenerated species should be potential independent and rapid under these conditions. However, photoreductions of solution species were observed for solution species lying negative of the CB edge; the data are summarized in Fig. 5 and Table I. Consider the behavior of anthracene (A) (Fig. 4). The small rise in the reduction current of A on p-GaAs starts at about -1.9V in the dark and on scan reversal a small anodic peak was observed at about -1.3V. When illuminated with red light a photoreduction current was observed at -1.6V with the appearance of the blue radical anion, A$^{\dot{-}}$, at the electrode surface. Thus the photoreduction peak potential is about 370 mV positive of its value on Pt. The background photoreduction of the solvent was also shifted from the

Downloaded 16 Feb 2009 to 146.6.143.190. Redistribution subject to ECS license or copyright; see http://www.ecsdl.org/terms_use.jsp

−2.5V observed on Pt to about −2V. The redox behavior of DPA was similar to that of A, with the oxidation of the radical anion shifted well positive of its $E°$ on Pt. The photoreduction peak potential was intensity dependent; at higher intensities both the cathodic and anodic peaks were shifted to more positive potentials. The cyclic voltammogram of DPA at the p-GaAs under a constant photon flux remained unchanged after more than 100 repetitive scans.

The cv behavior of $Ru(bipy)_3^{+2}$ on p-GaAs is shown in Fig. 10. The dark reduction occurs at very negative potentials with a small broad oxidation peak on reversal at potentials positive of V_{fb}. The photoreduction occurs well positive of its value on Pt. The reoxidation peak potentials under illumination were dependent on the switching potential. A more negative E_λ produced a larger concentration buildup of the reduced species and the reoxidation peak occurred at more negative potentials. Polycrystalline p-GaAs electrodes showed similar behavior to the single crystal with an observed underpotential on photoreduction of similar magnitude.

A hysteresis was observed in the *i-V* curves for the reduction of AQ on p-GaAs, which occurred in the dark 1.5V negative of its value on Pt. The oxidation of $AQ^{\overline{\cdot}}$ was very sensitive to surface conditions and the anodic peak height on reversal, in the dark, decreased on repetitive scans. The anodic peak height increased, however, when the electrode was illuminated for 2-3 sec between scans. The photoreduction peak potential occurred at potentials positive of its E_{pc} at Pt with etching procedure (D) (Fig. 6). No underpotential was observed, however, for etchants (B) and (C).

The unexpected photoeffects at p-GaAs found for reductions of couples with redox energies located above the conduction bandedge is analogous to the photoeffects observed with these couples at n-GaAs. Again the strong effect of etching pretreatment procedure, the observed crossing of the *i-V* curves, and effect of E_λ on E_{pa} all suggest that a surface layer is responsible for this behavior.

The behavior of p-GaAs with $Ru(TPTZ)_2^{+3}$ was similar to that of $Ru(bipy)_3^{+2}$ with the reoxidation peak potential of $Ru(TPTZ)_2^{+2}$ very positive of where the reduction of the +3 species occurs, and ∼0.2V positive of E_{pa} on Pt. The photoreduction of the +3 state started at about +0.1V and the reoxidation peak potentials depended on E_λ as previously described. A hysteresis of crossing of the *i-V* curve was observed during the dark cv reduction of BQ on reversal. Although the photoreduction current started at **−0.2V,** E_{pc} under illumination was negative of E_{pc} of BQ on Pt. Although the peak potential for the reduction of $Ox\text{-}1^+$ on p-GaAs occurred at potentials more positive than either BQ or $Ru(TPTZ)_2^{+3}$, the subsequent potential scans in the dark produced a more negative peak with a hysteresis observed. The photoreduction peak, as shown in Fig. 3, was observed on single crystal and polycrystalline in p-GaAs.

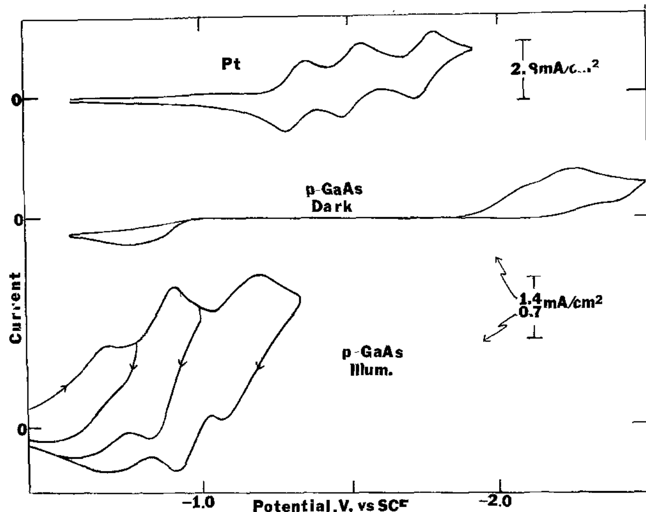

Fig. 10. Cyclic voltammogram at 0.2 V/sec of $Ru(bipy)_3^{+2}$ at a Pt disk electrode and single crystal p-GaAs electrode in the dark and illuminated with red light. The $Ru(bipy)_3^{+2}$ concentration was 1.2 mmoles.

The *i-V* curve for the reduction of Ox-1 to the radical anion and the underpotential developed on photoreduction are similar to the behavior previously described for redox couples with similar standard potentials as shown in Fig. 5.

The TMPD/$TMPD^{\overset{+}{\cdot}}$ redox potential lies very near the valence band of GaAs so that there is overlap of the oxidized species with the VB and hole injection into the VB is possible. Nearly reversible electron transfer occurs in the dark and only a very small photoreduction current is seen, when the electrode is illuminated with red light.

Discussion

An important feature of the behavior of GaAs electrodes which differs from other electrodes studied previously in ACN is the occurrence of specific surface effects. When the GaAs electrode is brought to negative potentials, reduction of the electrode surface occurs. The surface layer so produced leads to shifts in the potentials for dark reductions of couples with standard potentials located negative of −1.0V (V_{fb} on n-GaAs) as well as photoeffects in the oxidation of these couples at n-type GaAs and in the reduction of these couples on p-type GaAs. Moreover, while the potential range at which photoeffects are observed is usually somewhat smaller than the semiconductor bandgap, for GaAs photoeffects occur over a potential range of at least 2.5V. For example, photooxidations of both anthracene radical anion ($E_{1/2}$(Pt) = −1.9V) and TMPD ($E_{1/2}$(Pt) = +0.1V) take place at n-GaAs (see Fig. 5); similarly photoreductions at p-GaAs over a region larger than E_g are found. Clear additional evidence that this effect involves formation of a surface layer is the occurrence for first scans toward negative potentials of freshly etched GaAs electrodes of a reduction wave with an integrated area corresponding to greater than monolayer coverage (*i.e.* > 15 μC), as well as the hysteresis observed in the *i-V* curves and the dependence of E_p on switching potential with several couples. Surface layers were proposed with the III-V gallium-containing semiconductor n-GaP (5, 20); however, n-GaP photoeffects were different than those found with n-GaAs with underpotentials observed with only a few redox species (5). Aqueous studies of the reduction process of n-GaAs have shown the production of AsH_3 when H_2 was evolved at the surface (21, 23).

The observed effects can be explained if this surface layer is assumed to form a Schottky junction with the underlying semiconductor analogous to a metal/semiconductor junction. Such a junction on the surface of the semiconductor could produce a barrier to electron flow in the dark and aid in electron transfer through the development of a photopotential when the junction is illuminated (Fig. 11). The photopotential would add in series to the applied potential, in such a direction as to assist reductions for p-type GaAs and assist oxidations at n-type GaAs. We attempted to obtain direct evidence for the existence of such a surface layer by comparison of the x-ray photoelectron and Auger electron spectroscopy of freshly etched and reduced GaAs electrode surfaces. The results were ambiguous, however, because large oxygen and carbon peaks were found on all surfaces making quantitative surface analysis difficult. Similar effects have previously been found in the electron spectroscopy of GaAs (24). Although slightly higher atomic ratios of Ga/As were found with the reduced material compared to etched GaAs, the large relative error in the analysis makes

Downloaded 16 Feb 2009 to 146.6.143.190. Redistribution subject to ECS license or copyright; see http://www.ecsdl.org/terms_use.jsp

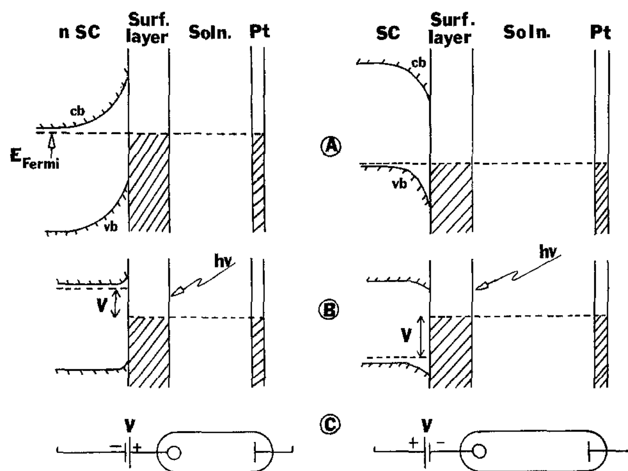

Fig. 11. Illustration of semiconductor in contact with solution and Pt counterelectrode (A) in equilibrium where the Fermi level (---) in each phase is equal. (B) Illumination of the semiconductor surface and photovoltage, V, between the semiconductor and surface layer and (C) equivalent electrochemical representation.

this finding inconclusive. The ratios of Ga/As on freshly etched GaAs surfaces [procedure (B)] were similar to those reported previously (0.78-0.85) (24), however.

A quantitative treatment of the observed electrochemical behavior is particularly difficult for GaAs, since the observed current depends not only on the usual mass transfer rates and electrode kinetics but also on the changing electrode surface. Thus the cv potentials were dependent on scan rate, light intensity, sweep direction, switching potential, and previous history of the electrode surface. The redox behavior of DPA, $Ru(bipy)_3^{+2}$, and $Ru(TPTZ)_2^{+3}$ on n-GaAs, where the peak potentials changed with switching potential, can be attributed to a decreased rate of reduction through the surface barrier and an increase of the anodic photocurrent under illumination. Abnormal peak potentials and peak separations are found, for example, with DPA (Fig. 3) where the increase of the anodic photocurrent and the decrease of cathodic current when a surface layer is formed at negative potentials produces the unusual situation of E_{pa} which is more negative than E_{pc}.

A second aspect of this investigation is a comparison of the electrochemical behavior at n-type and p-type material of couples whose solution energy levels are located within the gap region. In the absence of surface states or intermediate levels, which can cause deviations from the predicted charge transfer behavior across an ideal semiconductor liquid interface (1), the rate of charge transfer from one phase to another is proportional to the density of filled states in one phase and acceptor states in the other. Ideally, in the absence of concentration polarization the rate of charge transfer across the semiconductor-solution interface to couples in the gap region is proportional to the surface concentration of electrons (in the CB), n_s, or holes (in the VB), p_s, given under equilibrium conditions by (1)

$$n_s = N_c \exp\{(E_F - E_C)/kT\} \quad [3]$$

$$p_s = N_v \exp\{-(E_F - E_V)/kT\} \quad [4]$$

where n_s and p_s are the surface concentration of electrons at the CB edge and holes at the VB edge, respectively; N_c and N_v are the effective density of states in the CB and VB, respectively; E_F is the position of the Fermi level; k is the Boltzmann constant; T is the absolute temperature. When E_F is within the bandgap region, then n_c and p_s are independent of the type (n- or p-) and amount of dopant. Thus, the rate of electron transfer in the absence of degeneracy across a chemically stable semiconductor-solution interface would be dopant independent (1). However, the peak potentials for reduction and reoxidation of solution species whose $E°$'s lie within the bandgap, such as BQ, Ox-1$^+$, and TMPD$^{\dot{+}}$ are different for n- and p-GaAs. Several sources of deviations from the simple model are possible which may explain the experimental results. First, thermal equilibrium, which is assumed within the semiconductor, may not exist at all current densities. The equilibrium concentration of minority carriers, as given by the Fermi distribution function, must be thermally generated and maintained at all potentials and current densities. It is generally accepted that thermal equilibrium cannot be maintained in larger bandgap semiconductors, such as n-TiO_2, when the electrode potential is made more positive than the middle of the bandgap (1). Second, electron transfer via intermediate levels (5) may occur through population of such levels by either the CB (in n-type) or VB (in p-type). Thus, the involvement of the CB or VB, where the concentrations of electrons and holes are dopant dependent would produce different currents for n- and p-GaAs. We might note that analogous studies showed the photodissolution of the n-GaAs in aqueous solutions at potentials very near those found here for the reduction of TMPD$^{\dot{+}}$ (via an intermediate level) (*i.e.*, −0.7V *vs.* SCE) (10, 12). The photoreduction and dark oxidations on p-GaAs were also shifted near this potential.

Finally, note (Table I) that large differences in E_{pc} were observed both in the dark and under illumination, for redox systems with a similar $E°$ (*e.g.*, Ox-1$^{\dot{+}}$ and BQ). Such large differences are not usually observed and the reasons for the effect are not clear. Possibly a specific interaction of the radical anions and cations with the GaAs occurs.

In agreement with previous studies of small bandgap n- and p-type Si electrodes in ACN, we found that mechanical polishing of the electrode surface without subsequent etching produced an electrode which showed metallic characteristics and greatly reduced photoeffects. Presumably this polishing produces a great many surface states which can mediate electron transfer to solution species in the dark and act as recombination centers for photogenerated electron-hole pairs.

Clearly, the surface effects observed complicate the behavior of GaAs electrodes. We might note, however, that these surface films can be stable and make possible the construction of rather efficient solar cells using n- and p-type GaAs (25), as well as systems for light energy up-conversion (26).

Acknowledgment

The support of this research by the National Science Foundation and The Electrochemical Society (by an Edward Weston Fellowship to P.K.) is gratefully acknowledged.

Manuscript received June 5, 1978.

Any discussion of this paper will appear in a Discussion Section to be published in the December 1979 JOURNAL. All discussions for the December 1979 Discussion Section should be submitted by Aug. 1, 1979.

Publication costs of this article were assisted by The University of Texas at Austin.

REFERENCES

1. (a) H. Gerischer, in "Physical Chemistry: An Advanced Treatise," Vol. 9A, H. Eyring, D. Henderson, and W. Jost, Editors, Academic Press, New York (1970); (b) H. Gerischer, *Adv. Electrochem. Eng.*, **1**, 139 (1961).
2. M. Tomkiewicz, in "Semiconductor Liquid-Junction Solar Cells," A. Heller, Editor, p. 92, The Electrochemical Society Softbound Symposium Series, Princeton, N.J. (1977).

Downloaded 16 Feb 2009 to 146.6.143.190. Redistribution subject to ECS license or copyright; see http://www.ecsdl.org/terms_use.jsp

3. A. Yamamoto and S. Yano, *This Journal*, **122**, 260 (1975).
4. R. A. L. Vanden Berghe, W. P. Gomes, and F. Cardon, (a) *Ber. Bunsenges. Phys. Chem.*, **77**, 289 (1973), (b) *ibid.*, **78**, 331 (1974).
5. P. A. Kohl and A. J. Bard, *J. Am. Chem. Soc.*, **99**, 7531 (1977).
6. S. N. Frank and A. J. Bard, *ibid.*, **97**, 7427 (1975).
7. D. Laser and A. J. Bard, *J. Phys. Chem.*, **80**, 459 (1976).
8. A. J. Bard and P. A. Kohl, in "Semiconductor Liquid-Junction Solar Cells," A. Heller, Editor, p. 222, The Electrochemical Society Softbound Symposium Series, Princeton, N.J. (1977).
9. K. C. Chang, A. Heller, B. Schwartz, S. Menezes, and B. Miller, *Science*, **196**, 1097 (1977).
10. A. B. Ellis, J. M. Bolts, S. W. Kaiser, and M. S. Wrighton, *J. Am. Chem. Soc.*, **99**, 2848 (1977).
11. K. Nobe, G. L. Bauerle, and M. Braun, *J. Appl. Electrochem.*, **7**, 379 (1977).
12. S. Gourgaud and D. Elliott, *This Journal*, **124**, 102 (1977).
13. P. A. Kohl, S. N. Frank, and A. J. Bard, *ibid.*, **124**, 225 (1977).
14. R. N. Noufi, P. A. Kohl, S. N. Frank, and A. J. Bard, *ibid.*, **125**, 246 (1978).
15. E. C. Dutoit, R. L. Van Meirhaeghe, F. Cardon, and W. P. Gomes, *Ber. Bunsenges. Phys. Chem.*, **79**, 1206 (1975).
16. W. H. Laflere, R. L. Van Meirhaeghe, F. Cardon, and W. P. Gomes, *Surf. Sci.*, **59**, 401 (1976).
17. W. H. Laflere, F. Cardon, and W. P. Gomes, *ibid.*, **44**, 541 (1974).
18. T. Ambridge and M. M. Faktor, *J. Appl. Electrochem.*, **4**, 135 (1974).
19. V. A. Myamlin and Y. V. Pleskov, "Electrochemistry of Semiconductors," Plenum Press, New York (1967).
20. (a) R. Landsberg, P. Janietz, and R. Dehmlow, *Z. Phys. Chem. (Leipzig)*, **257**, 657 (1976); (b) *J. Electroanal. Chem.*, **65**, 115 (1957); (c) *Z. Chem.*, **15**, 38, 106 (1975); (d) *ibid.*, **14**, 363 (1974).
21. H. Gerischer, and I. Mattes, *Z. Phys. Chem. N.F.*, **49**, 112 (1966).
22. H. Gerischer, *Ber. Bunsenges. Phys. Chem.*, **69**, 578 (1965).
23. H. Gerischer, *Electrochim. Acta*, **13**, 1329 (1968).
24. C. C. Chang, P. H. Citrin, and B. Schwartz, *J. Vac. Sci. Technol.*, **14**, 943 (1977).
25. P. A. Kohl and A. J. Bard, Unpublished data.
26. J. D. Luttmer and A. J. Bard, Unpublished data.

Structure Sensitivity in the Electrocatalytic Properties of Pt

I. Hydrogen Adsorption on Low Index Single Crystals and the Role of Steps

Philip N. Ross, Jr.[1]

United Technologies Research Center, East Hartford, Connecticut 06108

ABSTRACT

Single crystal surfaces were used to examine the structure sensitivity of hydrogen chemisorption on Pt in dilute acid electrolyte. An electrochemical cell was coupled directly with an ultrahigh vacuum system, and low energy electron diffraction (LEED) and Auger electron spectroscopy (AES) were used to determine the structure and composition of the electrode surfaces. Hydrogen adsorption was examined by triangular sweep cyclic voltammetry. Contributions to the multiple peaks observed in voltammograms of Pt due specifically to anions were deduced and the effects of surface geometry alone were determined. A difference in hydrogen bond energy (3.4 kcal/mole) was observed for hydrogen on the (111)-(1 × 1) and the (100)-(1 × 1) surface. Hydrogen was also found to be more strongly bound at (~4 kcal/mole) at (100) steps than on the atomically flat (100) surface. Hydrogen adsorption on highly ordered surfaces could be described quantitatively by the classical model for single site adsorption on a homogeneous surface with a weak interaction between nearest neighbor pairs. This repulsive interaction lowers the coverage at 0V (NHE) of hydrogen on a perfect (111) surface to less than a monolayer. Some evidence is presented suggesting that anion adsorption is also structure sensitive and that the "third" anodic peak observed on Pt polycrystals in 1*N* H_2SO_4 is due to structure-sensitive anion adsorption.

Single crystal surfaces of controlled and known structure can be used to isolate the effect of site geometry on the electrocatalytic properties of electrode surfaces. Of particular practical importance is the determination of site specificity in the electrocatalytic properties of small (~ 1 nm) clusters of metal atoms, such as one has in the case of highly dispersed Pt on carbon (1). The geometry of the surface atoms in these clusters depends on the packing geometry, the number of atoms in the cluster, and the shape of the clusters, *e.g.*, octahedrons, cubo-octahedrons, icosohedrons, etc. Various thermodynamic calculations have been proposed (2-4) to predict the equilibrium cluster geometry as a function of the number of atoms per cluster, but there is at this time no experimental confirmation of any of these models. It is possible, however, to simulate nearly all of the different surface coordinations which may occur on clusters by the use of single crystals and to learn *a priori* whether cluster geometry has an important effect on catalytic properties.

In this work, single crystals are used to isolate structure sensitivity in the electrocatalytic properties of Pt surfaces in aqueous acid electrolyte. In Part I, the sensitivity of the Pt-H_{ads} bond energy to the surface structure is studied using the low index surfaces of (111) and (100) orientations and a stepped surface with a high periodicity of monatomic steps prepared from a single crystal of (211) orientation. These same surfaces are used in Part II (5) in the study of the

[1] Present address: Lawrence Berkeley Laboratories, Materials and Molecular Research Division, Berkeley, California 94730.

Key words: Auger electron spectroscopy, low energy electron diffraction, stoichiometry of hydrogen on Pt.

Downloaded 16 Feb 2009 to 146.6.143.190. Redistribution subject to ECS license or copyright; see http://www.ecsdl.org/terms_use.jsp